INTERNATIONAL ATOMIC ENERGY AGENCY
UNITED NATIONS EDUCATIONAL, SCIENTIFIC AND CULTURAL ORGANIZATION
INTERNATIONAL CENTRE FOR THEORETICAL PHYSICS
I.C.T.P., P.O. BOX 586, 34100 TRIESTE, ITALY, CABLE: CENTRATOM TRIESTE

UNITED NATIONS INDUSTRIAL DEVELOPMENT ORGANIZATION

INTERNATIONAL CENTRE FOR SCIENCE AND HIGH TECHNOLOGY
c/o INTERNATIONAL CENTRE FOR THEORETICAL PHYSICS 34100 TRIESTE (ITALY) VIA GRIGNANO, 9 (ADRIATICO PALACE) P.O. BOX 586 TELEPHONE 040-224572 TELEFAX 040-224575 TELEX 460449 APH I

SMR.648 - 46

SECOND AUTUMN WORKSHOP ON MATHEMATICAL ECOLOGY

(2 - 20 November 1992)

"Chaos and Biological Complexity in Measles Dynamics"

B.T. Grenfell
Department of Zoology
Cambridge University
Cambridge CB2 3EJ
U.K.

These are preliminary lecture notes, intended only for distribution to participants.

EPIDEMIOLOGY

- Cycles (linear)
- Persistence
- Stochasticity
- Age structure
- Spatial structure

- VACCINATION
  cycles
  eradication threshold

NONLINEAR DYNAMICS

- Cycles (nonlinear)
- Stochasticity
- Nonlinear predictability

CHAOS AND BIOLOGICAL COMPLEXITY IN MEASLES DYNAMICS

Running head: Complexity and measles dynamics
(3200 words)

by
B. M. Bolker
B. T. Grenfell

Department of Zoology, Cambridge University
Downing St., Cambridge CB2 3EJ
Telephone: (0223) 334430
Fax: (0223) 336676

SUMMARY

Measles epidemiology offers a useful perspective on the construction of models to describe the dynamics of ecological systems. Simple models of measles transmission can generate deterministic chaos by various mechanisms (Schwartz, 1985; Aron & Schwärtz, 1984; Rand & Wilson, 1991). However, incorporating more biological realism into the model, in the form of age-structure and realism in the seasonal forcing function (Schenzle, 1984), can suppress complex dynamics. Adding stochastic terms to the models restores complex dynamics, but raises new questions about demographic scale and population structure in these models.

I. INTRODUCTION

Measles is among the best documented of human diseases in terms of epidemiology and population dynamics (Black, 1984; Anderson & May, 1991). The public health importance of measles has led to the collection of relatively long notification time series for measles in many developed countries (Fig. 1) (Anderson *et al.* 1984). The comparative simplicity of infection and immunity (Black, 1984) in measles also allows the construction of plausible epidemiological models. This combination of data and conceptual framework has generated a large quantitative literature examining the dynamics of the disease (Schaffer & Kot, 1985; Drepper, 1988; Olsen *et al.* 1988; Olsen & Schaffer, 1990). This work has focused mainly on describing the persistence of infection (particularly under the impact of mass vaccination) (Anderson & May, 1983; Anderson & May, 1985a; Tudor, 1985; Anderson & May, 1982; Anderson & May, 1985b) and accounting for the striking pattern of recurrent epidemics observed in developed countries (Soper, 1929; Hamer, 1906; Bartlett, 1957; London & Yorke, 1973; Anderson *et al.* 1984;

Fine & Clarkson, 1982) (Fig. 1). Both deterministic (Anderson & May, 1983; Olsen & Schaffer, 1990; Schenzle, 1984; Aron & Schwartz, 1984) and stochastic (Bartlett, 1960; Griffiths, 1973; Bartlett, 1957) formulations of measles models have contributed to this body of work.

The last decade has seen considerable development of epidemiological models for measles, to allow for various heterogeneities in transmission (spatial, demographic, genetic, etc. (Anderson & May, 1984; Murray & Cliff, 1975; Cairns, 1989)). In particular, models incorporating seasonality (Fine & Clarkson, 1982; London & Yorke, 1973; Olsen & Schaffer, 1990; Aron & Schwartz, 1984) and age structure (Anderson & May, 1985a; Dietz & Schenzle, 1985a; Schenzle, 1984; Tudor, 1985) generate important predictions both about the likely performance of vaccination strategies (Anderson & May, 1985a; Anderson & May, 1983; Cairns, 1989; Greenhalgh, 1988; Yorke *et al.* 1979) and the observed dynamics of infection (Olsen & Schaffer, 1990; Schenzle, 1984; Rand & Wilson, 1991).

Recently, much attention has also been focused on the possibility that measles dynamics in developed countries may exhibit low-dimensional chaos (Schaffer & Kot, 1985; Olsen *et al.* 1988; Olsen & Schaffer, 1990; Sugihara *et al.* 1990; Rand & Wilson, 1991; Grenfell, 1992a). The search for chaos is based on analyses of observed measles time series and data generated from a simple epidemiological model (the forced SEIR model) (Schwartz, 1985; Aron & Schwartz, 1984). Here, we show that adding more biological realism (in terms of age structure (Dietz & Schenzle, 1985b; Schenzle, 1984)) to the deterministic model reduces its propensity for chaos. Further analyses of stochastic analogues of the model also reveal a potentially intricate relationship between regularity and spatial scale in measles dynamics.

II. EPIDEMIOLOGICAL MODELS

SEIR model

Theoretical analyses have built on a simple compartmental framework, the well known SEIR (Susceptible/Exposed/Infectious/Recovered) model (Hamer, 1906; Soper, 1929; Kermack & McKendrick, 1927; Anderson & May, 1991; Dietz & Schenzle, 1985b). It is expressed as a set of three non-linear ordinary differential equations

$$\begin{aligned} \frac{dS}{dt} &= \mu N(1-p) - (\mu+\beta I)S \\ \frac{dE}{dt} &= \beta IS - (\mu+\sigma)E \\ \frac{dI}{dt} &= \sigma E - (\mu+\gamma)I \end{aligned} \qquad (1)$$

S, E, I and R respectively represent the density of Susceptible, Exposed, Infectious and Recovered individuals, in a constant total population of size N=S+E+I+R. Average life expectancy, disease incubation, and infectious periods are $1/\mu$, $1/\sigma$, and $1/\gamma$ respectively, while the infection rate of susceptibles by infectious individuals is controlled by the parameter β. Recently, this model has been refined to allow for various heterogeneities in transmission (β), particularly with respect to host age (Anderson & May, 1985a; Dietz & Schenzle, 1985b; Dietz, 1976; Schenzle, 1984; Tudor, 1985), seasonality in transmission (due mainly to the aggregation of children in schools) (Aron & Schwartz, 1984; Schaffer & Kot, 1985; Olsen *et al.* 1988; London & Yorke, 1973; Dietz, 1976; Schenzle, 1984), distribution of latent and infectious periods (Grossman, 1980), and spatial and genetic structure (Murray & Cliff, 1975; May & Anderson, 1984). The inclusion of seasonality and age structure has been particularly successful in modelling the regular biennial oscillation in measles cases in England and Wales before vaccination (Schenzle, 1984)

(Fig. 1*a*, 2*e*). However, some data sets show more irregular patterns, with some evidence of three-year cycles (Fig 1*c*,*d*,*f*).

These irregularities have also drawn the attention of ecologists and dynamicists (Schaffer & Kot, 1985; Olsen *et al.* 1988; Olsen & Schaffer, 1990; Sugihara & May, 1990; Rand & Wilson, 1991), who have brought a new dimension to the field by seeking chaos in observed measles time series and in data generated from models. The latter analysis has been based on the simple SEIR model (equations (1)), with the addition of a sinusoidal forcing term,

$$\beta(t)=b_0(1+b_1\cos(2\pi t)) \qquad (2)$$

This formulation undoubtedly generates chaotic dynamics for sufficiently large degrees of seasonal forcing, when seasonal amplitude (b_1) $\gtrsim 0.27$ (as illustrated by Fig. 2*a*,*c*) (Schaffer & Kot, 1985; Olsen *et al.* 1988; Olsen & Schaffer, 1990; Aron & Schwartz, 1984). However, there are biological objections to the large degree of seasonal forcing necessary to generate chaos (Pool, 1989) and the consequently small numbers of cases generated during epidemic troughs (Grenfell, 1992a) (for example 10^{-14} of population size in Fig. 2*a*). The inclusion of more realistic seasonal patterns (Kot *et al.* 1988; London & Yorke, 1973) and chaotic behaviour generated by noise (Rand & Wilson, 1991) mitigate these problems somewhat but do not eliminate them—stochastic analogues of the forced SEIR model show fadeouts of infection more than is observed in real datasets (Black, 1966; Bartlett, 1957; Bartlett, 1960; Grenfell, 1992a).

Realistic age-structured model (RAS)

A more realistic age-structured (RAS) model from the epidemiological literature (Schenzle, 1984) addresses some of the shortcomings of the SEIR model. Essentially, the model allows for the observed lower contact (and therefore infection) rate among pre-school children compared to primary school children during school terms, and recognizes the importance of school children and the pattern of school calendars in measles epidemiology (Schenzle, 1984; Fine & Clarkson, 1982; Anderson & May, 1985a). The RAS model is (to our knowledge) the only model in the literature that incorporates both age-structure and seasonal structure. The RAS model preserves the basic compartment structure of the SEIR model, and the simplified biology of the measles-host interaction (including the constant latency and recovery rates σ and γ), but adds realistic structure to the spread of infection between hosts.

The RAS model divides the population into 21 *age cohorts* representing people aged 0-1, 1-2, ..., and 21 and older. Newborn children flow continuously into cohort 1, but the members of each cohort advance discontinuously to the next cohort at the beginning of the model year, which corresponds to the beginning of the school year. The *per capita* mortality rate μ is zero in the first 20 cohorts, and constant in the last cohort. (The birth rate B and death rate determine the (constant) population size: $N=B/(20+(1/\mu))$). The cohorts fall in turn into four *age classes*, representing pre-school children (cohorts 1-5), primary school children (6-10), adolescents (11-20) and adults (21).

Figure 2*a* shows the pattern of cross-contact among different age classes during the school term; primary-school children meet (and infect) each other at a very high rate, primary-school children meet primary-school children at a lower but still significant rate, and adolescents and adults meet at lower rates. The symmetry of this "who acquires

infection from whom" (WAIFW) matrix allows us to calculate the equilibrium contact rate parameters from age-structured case reports or serological data (Anderson & May, 1985a). (These parameters served as a starting point for finding the set of parameters that best fit the average biennium derived from the England and Wales dataset.)

Outside school terms, when primary-school children are not aggregated in schools, all pre-school and primary-school children mix at the same relatively low rate. The specific pattern of the English school calendar acts as the seasonal input, faithfully reproducing the observed changes in contact rate during school holidays. Thus the RAS model carefully includes the most important heterogeneities neglected by the SEIR model.

III. MODEL DYNAMICS

Deterministic models

The dynamic behaviour of the SEIR and RAS models is qualitatively different (Fig. 2). In contrast to the transition to chaos of the SEIR model with increasing seasonality, the RAS model shows a short and simple bifurcation sequence ending in a collapse to a simple annual cycle. The key to this difference is apparent in comparing the minimum number of infectives generated by the two models (contrast the bifurcation diagrams in Fig. 2*a*, SEIR, and Fig. 2*d*, RAS). Essentially, large-amplitude chaos in the forced SEIR model is associated with the divergence of nearby states in the deep troughs between epidemics (Drepper, 1988) - the RAS model never allows the number of infectives to fall low enough for this large-amplitude chaos to manifest itself. (Preliminary analyses of deterministic models with delays rather than constant recovery rates (Grossman, 1980) suggest that these models exhibit qualitatively similar dynamics.)

The absence of deep troughs (and therefore chaos) in the RAS model arises from

the more realistic assumptions that it makes about heterogeneities in transmission (Fig. 3*a*). Specifically, the relatively low (and constant) contact rate between pre- and primary-school children protects the pre-school group from the violent epidemics experienced by children when they go to school. This protection allows them to act as a reservoir of infectives in the troughs between epidemics, as long as the pre-school contact rate is sufficiently high (for (unrealistically) low pre-school contact rates, chaos emerges). In consequence, the relative proportion of pre-school cases *rises* during interepidemic troughs, compared to the constant proportion to be expected from the homogeneous SEIR model (Fig. 3*b*). The observed data for England and Wales also show a strong biennial pattern which agrees qualitatively with the RAS model (Fig. 3*b*). In more detail, the RAS model predicts a greater amplitude for the pre-school pattern than is observed, suggesting further room for biological refinement in the model (in terms of contact structure, temporal variation, etc.). (Note, however that the fit of the RAS model to total reported cases is nevertheless very close (Fig. 2*e*).)

Stochastic models

The preceding results are based on deterministic models. Recently, however, Rand and Wilson (1991) have pointed out the important result that interactions between environmental or demographic noise and the nonlinearity of the SEIR model can sustain transient chaotic behaviour. The addition of moderate amounts of environmental noise to the RAS model does not *qualitatively* affect its dynamics (Fig. 4*a*); remnants of the deterministic bifurcation structure (Fig. 1*d*) are still visible. (The detailed global dynamics of the RAS model and their interactions with stochasticity warrant more study, but here we concentrate on the generic aspects and biological implications of the dynamics.) The

impact of demographic noise (which has an important place in the study of measles (Bartlett, 1957; Bartlett, 1960)) can generate more complex dynamics, as illustrated by Monte Carlo simulations (Fig. 4*b*,*c*). The Monte Carlo method (Bartlett, 1960; Bartlett, 1961; Murray & Cliff, 1975; Anderson & May, 1986; Anderson & May, 1991; Olsen *et al.* 1988) takes an analogue of the equations governing the deterministic dynamics and assumes that each process (birth, infection, etc.) occurs at a constant probability over time and thus can be modelled by choosing deviates from an exponential distribution with appropriate mean.

For large (country-wide) populations (possibly corresponding to England and Wales, which may have represented a single epidemiologic unit before the start of mass vaccination (Fine & Clarkson, 1982)), addition of demographic noise generates the expected result of noise around the biennial pattern, but, again, no qualitative effect on the dynamics (Fig. 4*b*).

The situation for smaller population sizes (corresponding to a city of one million) is more complex (Fig. 4*c*). The regular biennial epidemics of the deterministic RAS model now break down into domains of irregular one- and two-year cycles interspersed with large-amplitude three-year oscillations. These results can also qualitatively be generated by the simple SEIR model (Schaffer *et al.* 1991). They show that significant amounts of demographic noise (operating at smaller population sizes and therefore spatial scales) can generate complex behaviour in the RAS model and in particular alternating periods of two-year and longer term cycles. The corresponding spectra for these periods (Fig. 4*c*, insets) show peaks at biennial and triennial frequencies, which corresponds with some of the observed data (Fig. 1*f*). The dynamic explanation for these different domains remains unclear. They may represent the operation of a chaotic repellor (Rand & Wilson,

1991) or some other dynamic object (Schwartz, 1985; Schaffer *et al.* 1991)—we are currently exploring these possibilities by examining the pattern of largest Lyapunov exponents (which reflect chaos and other sources of divergence (Rand & Wilson, 1991)) in the different domains. A further complication is that the three-year domain shows a high incidence of fadeout of infection, indicating that explicit spatial structure in the models may be necessary to characterize this behaviour properly.

Spatial structure may have profound effects on the dynamics of the models, particularly in the dynamically important epidemic troughs; small differences in epidemic timing between different areas could resolve the current difficulties with unrealistic levels of fadeout in seasonally forced models. In order to explore these problems, we are examining both data (from major cities in England and Wales) and spatially structured models. As yet, however, no model with both complicated dynamics and a realistic level of fadeout has come to light.

IV. CONCLUSION

Overall, these results illustrate the general point that introducing extra biological complexity into deterministic ecological models can simplify rather than complicate their behaviour, particularly if it reduces the propensity for extreme population fluctuations (Grenfell, 1992b). In terms of the dynamics of measles, it appears that the RAS model may represent the *minimum* amount of biological complexity required to explore the nonlinear dynamics of measles. The deterministic RAS model generates robust biennial cycles over a wide range of parameters, matching the pattern observed in England and Wales, but cannot generate the more complex longer-term patterns observed in other cities. With the introduction of demographic noise the RAS model does prove capable of

generating irregular, longer-term patterns. However, deciding whether these patterns represent the real mechanism underlying longer term cycles or are artifacts of fadeout will require models incorporating spatial structure. These complexities pose an interesting challenge to ecologists, nonlinear dynamicists, and epidemiologists alike.

ACKNOWLEDGEMENTS

We are most grateful to David Rand, Howard Wilson, Adam Kleczkowski, Robert May, and Lars Olsen for helpful discussions, and to the latter for kindly providing measles data for Copenhagen.

FIGURE CAPTIONS

1. Case reporting data and power spectra for various regions. *(a)* Weekly case reports, England and Wales, 1948-1966; *(b)* weekly case reports, Birmingham, 1948-1966 (both from the Registrar General's Weekly Reports); *(c)* monthly case reports, New York City, 1928-1964 (London & Yorke, 1973), *(d)* monthly case reports, Copenhagen, 1928-1968 (L.F. Olsen, pers. comm.). Spectra are smoothed using a 3-point running mean, and plotted as power against frequency ($year^{-1}$). The dotted line indicates 0.5 $year^{-1}$, the frequency of biennial cycles. *(e)* England and Wales, Birmingham (logged) power spectra, *(f)* New York City, Copenhagen (logged) power spectra. Note that the latter two spectra show evidence of components at long-term frequencies not equal to the biennial frequency (Olsen & Schaffer, 1990).

2. Bifurcation diagrams (*a,d*) and time series (*b,c,e*) of sinusoidally-forced SEIR and realistic age-structured (RAS) models. Bifurcation diagrams show $\log_{10}$(infectives) in a population of 50 million, sampled annually at the beginning of the epidemiologic year (September, near the minimum number of infectives) for 100 years after a 200-year transient, for given values of seasonal forcing amplitude. (A single point thus represents an annual cycle, two points a biennial cycle, and so on.) *(a)* SEIR bifurcation diagram (the model is formulated as $\beta = c_0 + c_1(1+\cos(2\pi t))$ rather than the more standard form in order to match the RAS bifurcation diagram more closely), $\log_{10}$(infectives) vs. c_1. (Parameters $N=5 \times 10^7$, $\mu=0.02$, $\gamma=73.0$, $\sigma=45.6$, $c_0 = 1.5 \times 10^{-5}$, $c_1 = 0$ to 9.0×10^{-5}, all units $year^{-1}$ except contact rate ($year^{-1}$ $infective^{-1}$)) *(b)* SEIR time series for the biennial regime, $c_1 = 8.5 \times 10^{-6}$ *(c)* SEIR time series for the chaotic regime, $c_1 = 2.0 \times 10^{-5}$ *(d)* Bifurcation diagram for the RAS model. This model is an age-structured extension of the

forced SEIR model, based on discrete age cohorts, as discussed in the text. The contact structure between age cohorts is shown in Figure 3*a*. Parameters are as given by Schenzle (1984): $N=5 \times 10^7$, $\mu=0.018$ person^{-1} year^{-1}, $B=666666$ year^{-1}, $\gamma=73.0$ year^{-1}, $\sigma=45.6$ year^{-1}. Contact parameters are the differences in rates between groups; b_4 = adult rate, b_3 = adolescent-adult, b_1 = pre-school-adolescent, b_2 = primary (during term)-pre-school. Contact rates are adjusted to give best least-squares fit to the England and Wales data (Fig. 2e): b_1=8.76e-6, b_2=0 to 5e-4, b_3=2.74e-6, b_4=4.38e-6 (year^{-1} infective^{-1})). Seasonal amplitude is b_2, the additional school-term contact rate among primary-school children. *(e)* RAS biennial time series; weekly case reports for contact rate parameters (b_1=8.76e-6, b_2=1.25e-4) giving best least-squares fit to case reporting data for England and Wales. The means (points) and standard errors (bars) for the (corrected) (Fine & Clarkson, 1982) weekly case reports from England and Wales, 1950-1964, are superimposed on the model output (line).

3. RAS model, age structure. *(a)* The "who acquires infection from whom" (WAIFW) matrix for the RAS model (Schenzle, 1984). Heights of bars represent relative contact rate for mixing between different age classes (pre-school (0-6 years), primary school (6-10 years), adolescent (10-20 years), adult (20 and older)). Note that the high within-primary school contact rate is only effective during school terms. During holidays within-primary school contact is at the same rate as the surrounding pre-school contact rates, as discussed in the text. *(b)* Fractions of total reported cases among children under 5 years in England and Wales, 1950-1964 (observed data from the Registrar General's Quarterly Summaries). The lines show the observed fractions, the fractions derived from RAS model simulations, and the (constant) fraction predicted from a homogeneous (non-age-structured) model.

Inset shows the normalized power spectrum (Chatfield, 1975) of the pre-school fraction for the data and the RAS model; (*) indicates a significant annual cycle ($p<0.001$ from the autocorrelation function) which cannot be generated by the homogeneous model. The spectra agree well, although the amplitude of the modelled time-series is larger than that observed, which suggests further room for biological refinement in the model.

4. *(a)* Bifurcation diagram for the RAS model (as described in Fig. 2) with 3% Gaussian noise. (The contact rate for each one-year age cohort is multiplied each week by a number picked from a normal distribution with mean 1.0 and variance 0.03; this method and parameters were picked for comparison with Rand and Wilson's results (1991) showing that 3% Gaussian noise added to the SEIR model excites chaotic transients with much larger amplitudes.) Parameters as in Fig. 2*d*. *(b)* Number of infectives over time, RAS stochastic (Monte Carlo) model for a large (country-wide) population: $N=5\times10^7$. The pattern is a noisy version of the biennial cycle seen in Fig. 2*d*. (Parameters as above.) *(c)* Time series of infectives for the RAS Monte Carlo model for a city of 1 million people: $N=10^6$. Parameters as above (except contact and birth rates scaled to new population size). **Insets** are power spectra of different dynamical domains showing 3-year and mixtures of 1- and 2-year cycles (the dotted line represents the biennial frequency). Spectral smoothing, etc., as in Fig. 1.

REFERENCES

Anderson, R.M., Grenfell, B.T. & May, R.M. 1984 Oscillatory fluctuations in the incidence of infectious disease and the impact of vaccination: time series analysis. *J.Hyg.(Camb.)*. **93**, 587-608.

Anderson, R.M. & May, R.M. 1982 Directly transmitted infectious diseases: control by vaccination. *Science*. **215**, 1053-1060.

Anderson, R.M. & May, R.M. 1983 Vaccination against rubella and measles: quantitative investigations of different policies. *J:Hyg.(Camb.)*. **90**, 259-325.

Anderson, R.M. & May, R.M. 1984 Spatial, temporal, and genetic heterogeneity in host populations and the design of immunization programmes. *IMA.J.Math.Appl.Med.Biol.* **1**, 233-266.

Anderson, R.M. & May, R.M. 1985a Age-related changes in the rate of disease transmission: implications for the design of vaccination programmes. *J.Hyg.(Camb.)*. **94**, 365-436.

Anderson, R.M. & May, R.M. 1985b Vaccination and herd immunity to infectious diseases. *Nature*. **318**, 323-329.

Anderson, R.M. & May, R.M. 1986 The invasion, persistence and spread of infectious diseases within animal and plant communities. *Phil.Trans.R.Soc.Lond.Biol.* **314**, 533-570.

Anderson, R.M. & May, R.M. 1991 *Infectious diseases of humans: dynamics and control.* Oxford University Press.

Aron, J.L. & Schwartz, I.B. 1984 Seasonality and period-doubling bifurcations in an epidemic model. *J.Theor.Biol.* **110**, 665-679.

Bartlett, M.S. 1957 Measles periodicity and community size. *J.Roy.Stat.Soc.A* **120**, 48-70.

Bartlett, M.S. 1960 The critical community size for measles in the U.S. *J.Roy.Stat.Soc.A* **123**, 37-44.

Bartlett, M.S. 1961 Monte Carlo studies in ecology and epidemiology. In *Proceedings of the Fourth Berkeley Symposium on Mathematical Statistics and Probability, vol. 4* pp. 39-55. Berkeley and Los Angeles: University of California.

Black, F.L. 1966 Measles endemicity in insular populations: critical community size and its evolutionary implication. *J.Theor.Biol.* **11**, 207-211.

Black, F.L. 1984 Measles. In *Viral Infections of Humans: Epidemiology and Control* (ed. Evans, A.S.) pp. 397-418. New York: Plenum.

Cairns, A.J.G. 1989 Epidemics in heterogeneous populations - aspects of optimal vaccination policies. *IMA.J.Math.Appl.Med.Biol.* **6**, 137-159.

Chatfield, C. 1975 *The analysis of time series: theory and practice.* London:Chapman and Hall.

Dietz, K. 1976 The incidence of infectious diseases under the influence of seasonal fluctuations. *Lect.Notes.Biomath.* 1-15.

Dietz, K. & Schenzle, D. 1985a Proportionate mixing models for age-dependent infection transmission. *J.Math.Biol.* **22**, 117-120.

Dietz, K. & Schenzle, D. 1985b Mathematical models for infectious disease statistics. In *A Celebration of Statistics* (ed. Atkinson, A.C. & Feinberg, S.E.) pp. 167-204. New York: Springer.

Drepper, F.R. 1988 Unstable determinism in the information production profile of an epidemiological time series. In *Ecodynamics: contributions to theoretical ecology* (ed. Wolff, W., Soeder, C.-J. & Drepper, F.R.) pp. 319-332. London: Springer-Verlag.

Fine, P.E.M. & Clarkson, J.A. 1982 Measles in England and Wales-I: an analysis of factors underlying seasonal patterns. *Int.J.Epidem.* **11**, 5-15.

Greenhalgh, D. 1988 Analytical threshold and stability results on age-structured epidemic models with vaccination. *Theor.Popul.Biol.* **33**, 266-290.

Grenfell, B.T. 1992a Chance and chaos in measles dynamics. *J.Roy.Stat.Soc.B.* **54**, 383-398.

Grenfell, B.T. 1992b Parasitism and the dynamics of ungulate grazing systems. *Am.Nat.* **139**, 907-929.

Griffiths, D.A. 1973 The effect of measles vaccination on the incidence of measles in the community. *J.Roy.Stat.Soc.A* **136**, 441-449.

Grossman, Z. 1980 Oscillatory phenomena in a model of infectious diseases. *Theor.Popul.Biol.* **18**, 204-243.

Hamer, W.H. 1906 Epidemic disease in England-the evidence of variability and of persistency of type. *Lancet.*

Kermack, W.O. & McKendrick, A.G. 1927 A contribution to the mathematical theory of epidemics. *Proc.R.Soc.Lond.A.* **115**, 700-721.

Kot, M., Graser, D.J., Truty, G.L., Schaffer, W.M. & Olsen, L.F. 1988 Changing criteria for imposing order. *Ecol.Modelling.* **43**, 75-110.

London, W.P. & Yorke, J.A. 1973 Recurrent outbreaks of measles, chickenpox and mumps. I. Seasonal variation in contact rates. *Am.J.Epidem.* **98**, 453-468.

May, R.M. & Anderson, R.M. 1984 Spatial heterogeneity and the design of immunization programs. *Math.Biosci.* **72**, 83-111.

Murray, G.D. & Cliff, A.D. 1975 A stochastic model for measles epidemics in a multi-region setting. *Inst.Brit.Geog.* **2**, 158-174.

Olsen, L.F., Truty, G.L. & Schaffer, W.M. 1988 Oscillations and chaos in epidemics: a nonlinear dynamic study of six childhood diseases in Copenhagen, Denmark. *Theor.Popul.Biol.* **33**, 344-370.

Olsen, L.F. & Schaffer, W.M. 1990 Chaos versus noisy periodicity: alternative hypotheses for childhood epidemics. *Science.* **249**, 499-504.

Pool, R. 1989 Is it chaos, or is it just noise? 1. *Science.* **243**, 25-28.

Rand, D.A. & Wilson, H. 1991 Chaotic stochasticity: a ubiquitous source of unpredictability in epidemics. *Proc.R.Soc.Lond.Biol.* **246**, 179-184.

Schaffer, W.M., Kendall, B.E. & Tidd, C.W. 1991 *Transient periodicity and episodic predictability in biological dynamics.* (Preprint)

Schaffer, W.M. & Kot, M. 1985 Nearly one dimensional dynamics in an epidemic. *J.Theor.Biol.* **112**, 403-427.

Schenzle, D. 1984 An age-structured model of pre- and post-vaccination measles transmission. *IMA.J.Math.Appl.Med.Biol.* **1**, 169-191.

Schwartz, I.B. 1985 Multiple recurrent outbreaks and predictability in seasonally forced nonlinear epidemic models. *J.Math.Biol.* **21**, 347-361.

Soper, M.A. 1929 The interpretation of periodicity in disease prevalence. *J.Roy.Stat.Soc.A* **92**, 34-61.

Sugihara, G., Grenfell, B. & May, R.M. 1990 Distinguishing error from chaos in ecological time series. *Phil.Trans.R.Soc.Lond.Biol.* **330**, 235-251.

Sugihara, G. & May, R.M. 1990 Nonlinear forecasting as a way of distinguishing chaos from measurement error in time series. *Nature*. **344**, 734-741.

Tudor, D.W. 1985 An age-dependent epidemic model with application to measles. *Math.Biosci.* **73**, 131-147.

Yorke, J.A., Nathanson, N., Pianigiani, G. & Martin, J. 1979 Seasonality and the requirements for perpetuation and eradication of viruses in populations. *Am.J.Epidem.* **109**, 103-123.

FIG 1

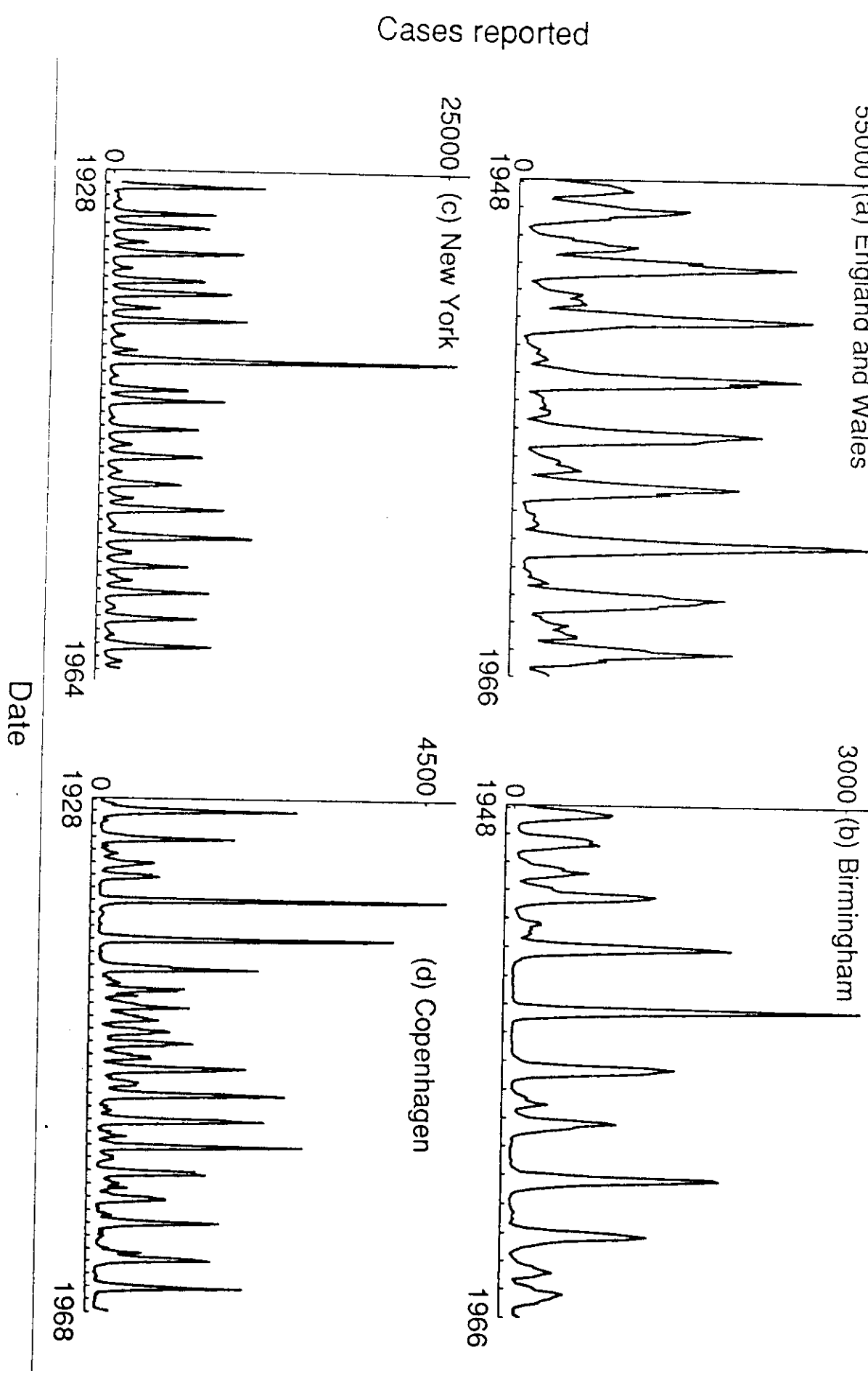
Cases reported
55000
(a) England and Wales
0
1948
1966
3000
(b) Birmingham
0
1948
1966
25000
(c) New York
0
1928
1964
4500
(d) Copenhagen
0
1928
1968
Date

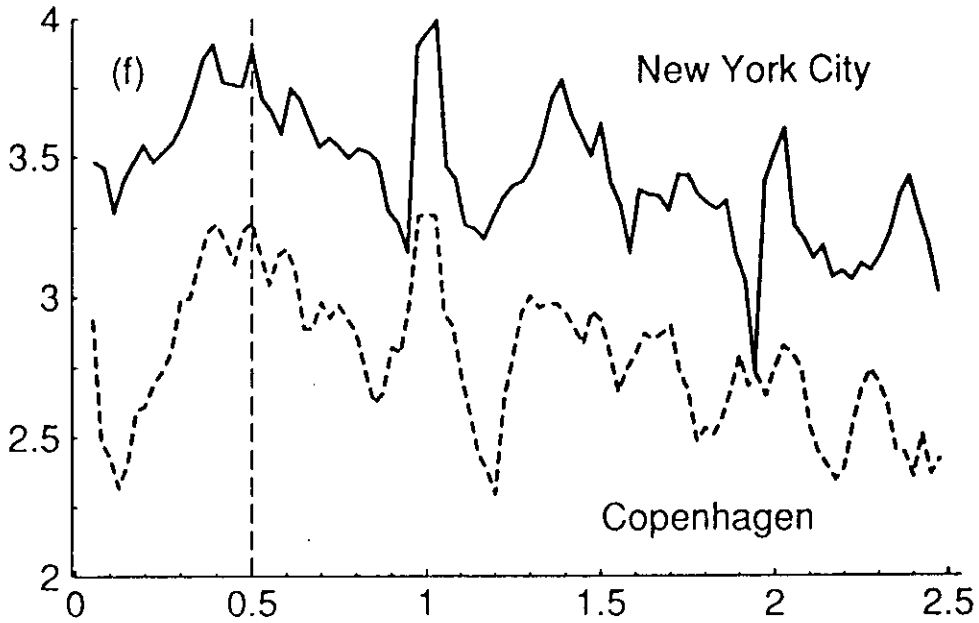
(f)
New York City
Copenhagen
4
3.5
3
2.5
2
0
0.5
1
1.5
2
2.5

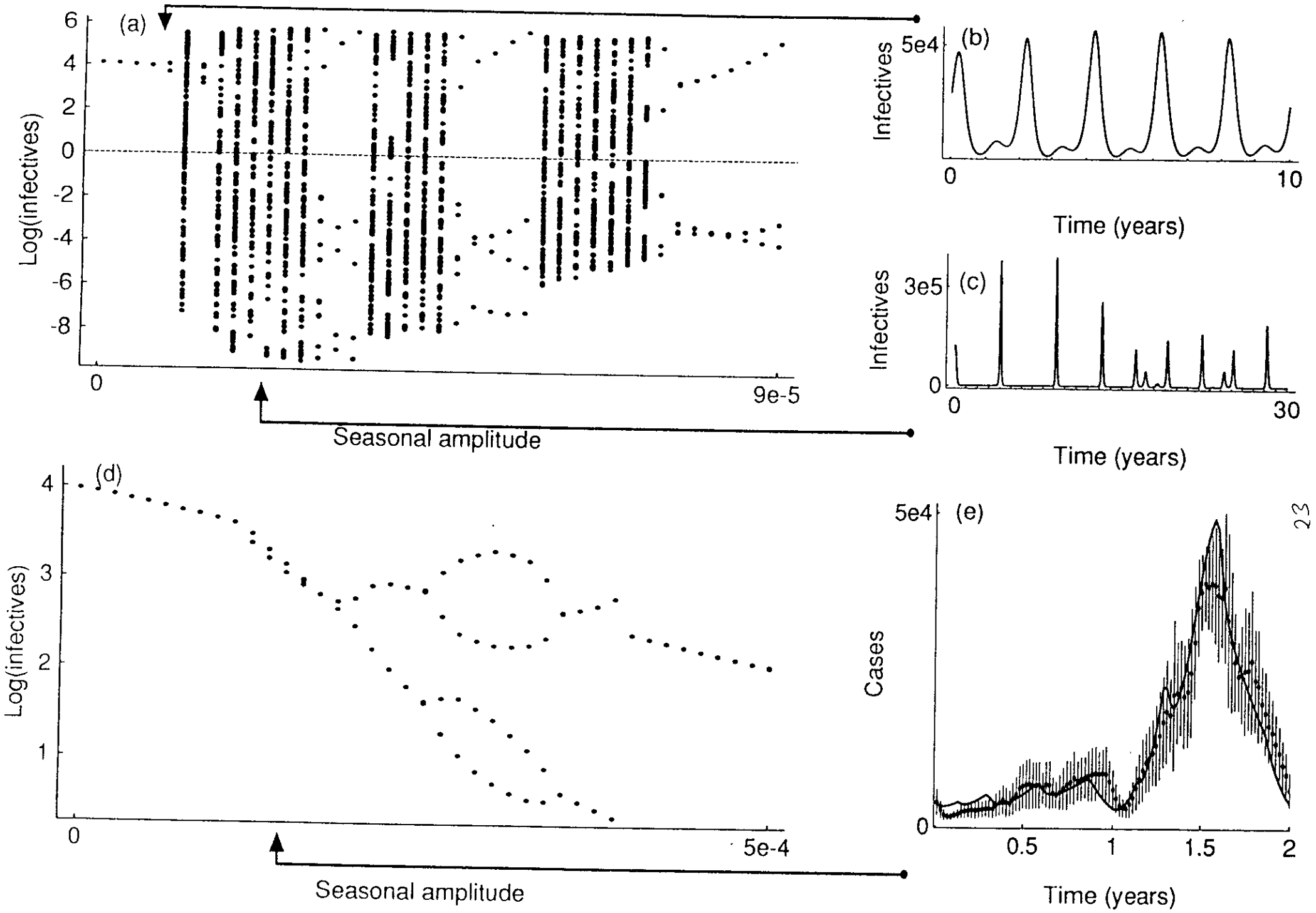
(a)
Log(infectives)
6
4
2
0
-2
-4
-6
-8
0
9e-5
Seasonal amplitude
(b)
Infectives
5e4
0
10
Time (years)
(c)
Infectives
3e5
0
0
30
Time (years)
(d)
Log(infectives)
4
3
2
1
0
5e-4
Seasonal amplitude
(e)
Cases
5e4
0
0.5
1
1.5
2
Time (years)

FIGURE 3

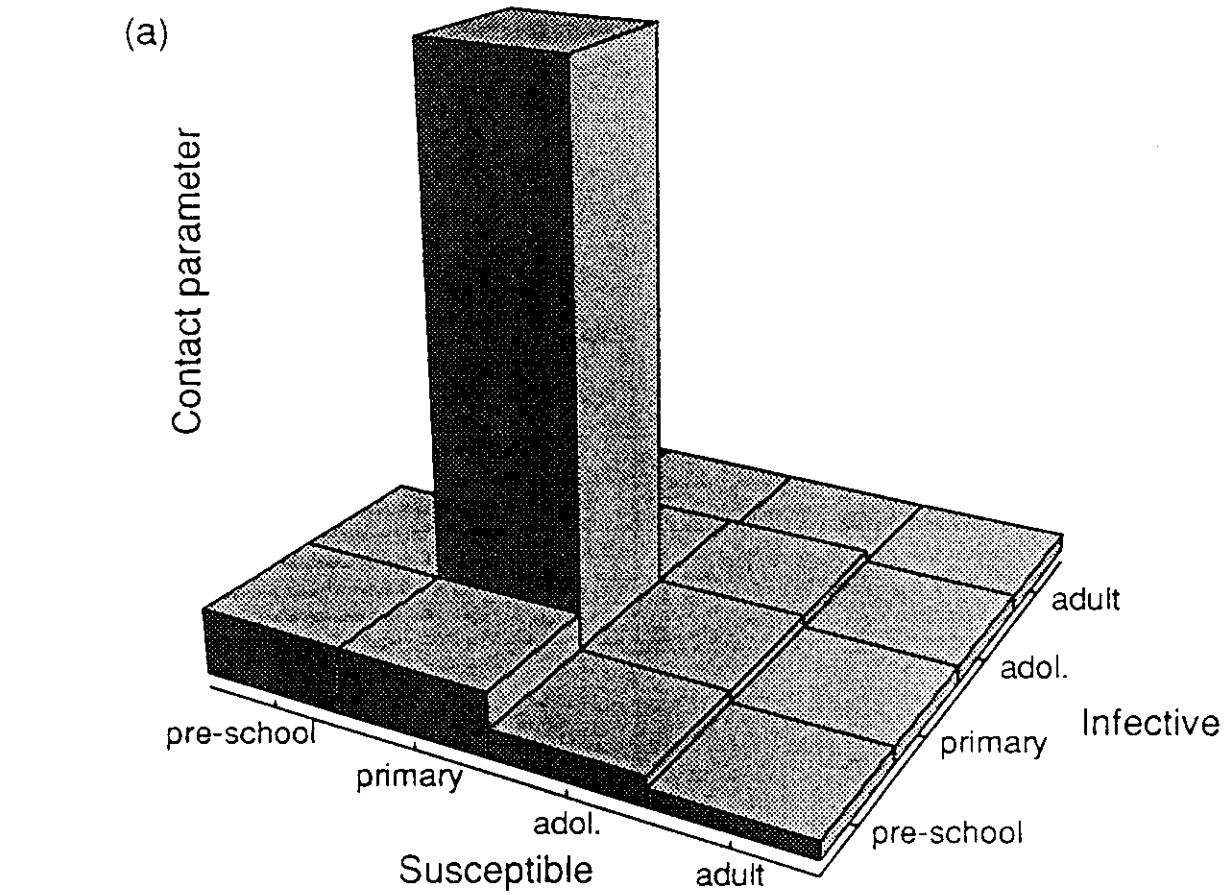
(a)
Contact parameter
pre-school
primary
adol.
adult
Susceptible
Infective
adult
adol.
primary
pre-school

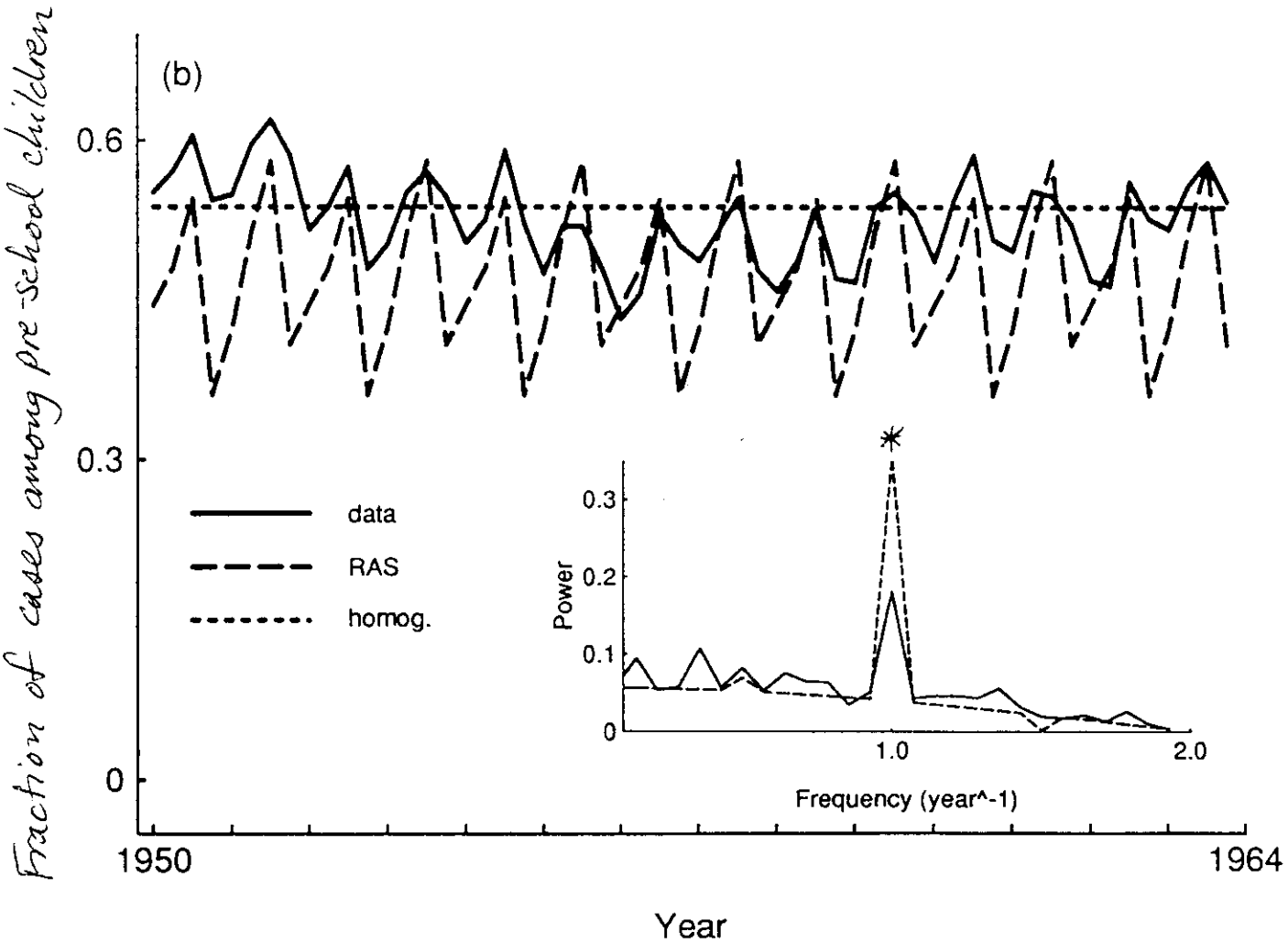
(b)
Fraction of cases among pre-school children
0.6
0.3
0
data
RAS
homog.
Power
0.3
0.2
0.1
0
1.0
2.0
Frequency (year^-1)
1950
1964
Year

FIGURE 4

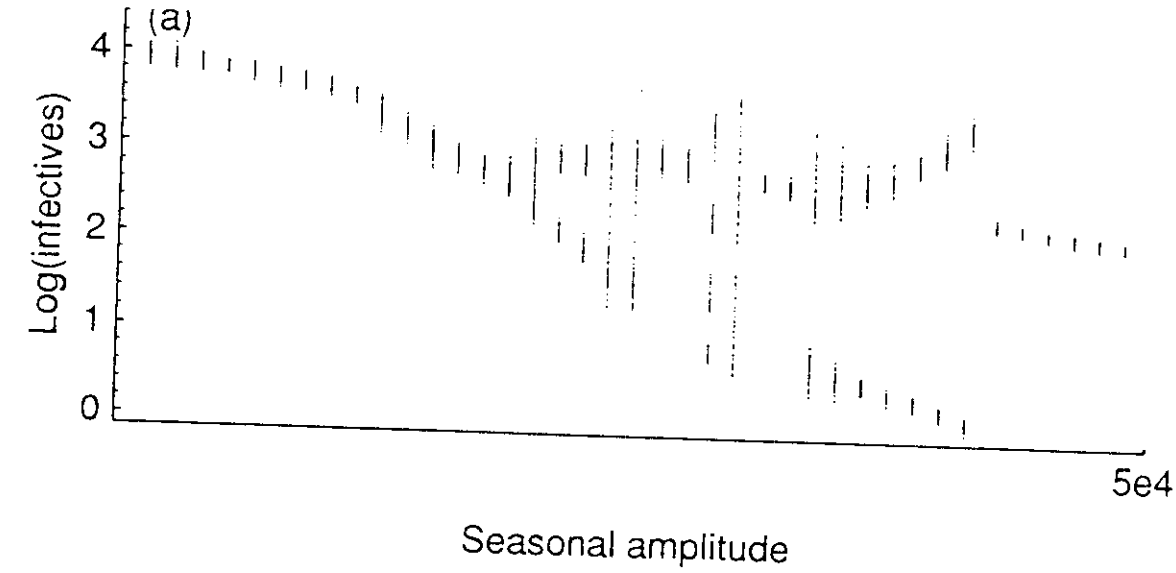
(a)
Log(infectives)
4
3
2
1
0
5e4
Seasonal amplitude

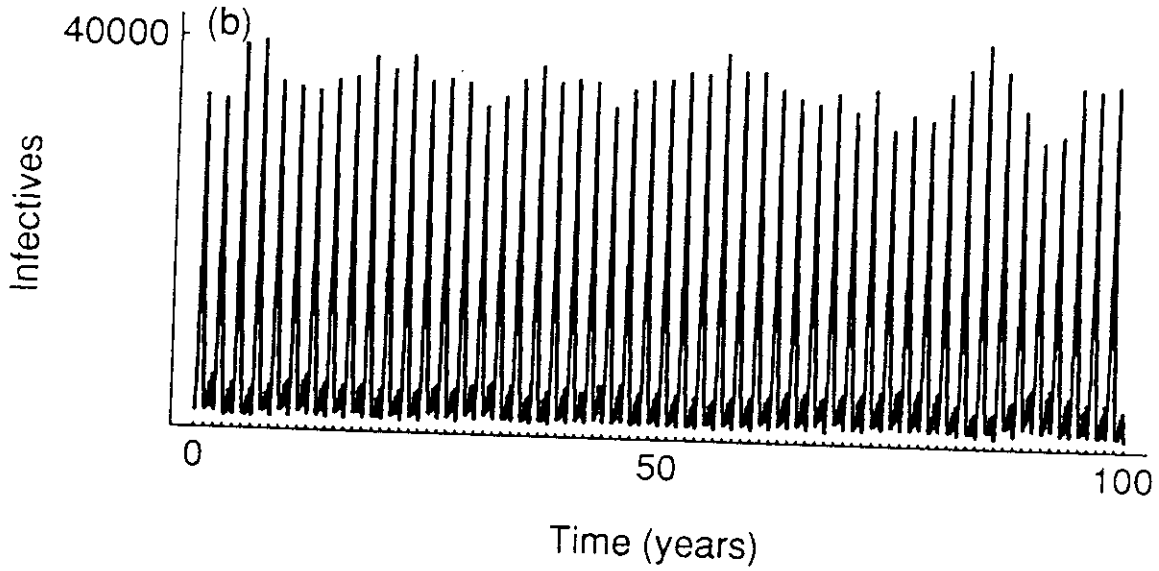
40000
(b)
Infectives
0
50
100
Time (years)

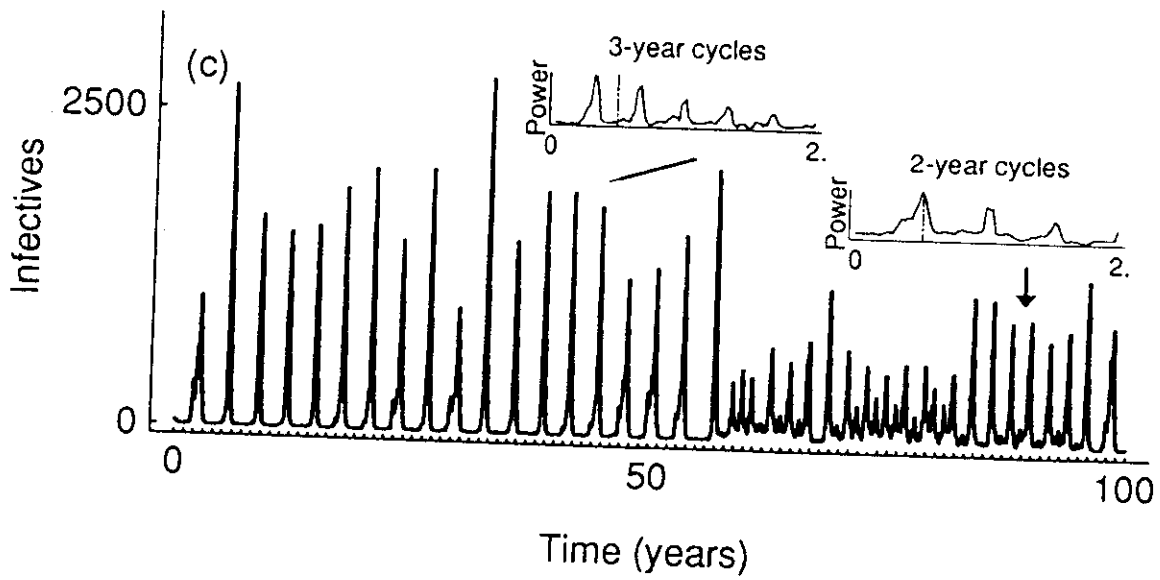
(c)
2500
Infectives
0
3-year cycles
Power
0
2.
2-year cycles
Power
0
2.
0
50
100
Time (years)